# SMART TAGS THAT ARE EXACTLY RELIABLE ENOUGH

Maaike M. Visser Taklo, Ph.D., Branson D. Belle, Daniel Nilsen Wright,
Astrid-Sofie B. Vardøy, Alexandre Garcia
SINTEF
Oslo, Norway
maaike.taklo@sintef.no

Torbjörn Eriksson, Olle Hagel, Magnus Danestig
Thin Film Electronics AS (Thinfilm)
Oslo, Norway
torbjorn.eriksson@thinfilm.no

**ABSTRACT**
Smart tags for fast moving consumer goods are among the products predicted to be part of the Internet of Everything. The tags must be extremely low cost, be fabricated in huge volumes, and have a quality accepted by the end user.

Screening tests have been performed to evaluate technologies for hybrid integration of smart tags. An anisotropic conductive adhesive (ACP) was compared with use of a low temperature solder and critical factors limiting the quality of each technology were identified. The motivation for the research was to avoid over-engineering of the quality of the joints where this would correlate with too high costs. For the system with an ACP, the matrix material was identified as the critical factor whereas for the soldered system, the quality of the backplane appeared more critical than the soldered joints themselves. Draft specifications that were considered in this work were not met for the system with ACP whereas they were easily met for all tested soldered systems.

Key words: Printed electronics, hybrid integration, anisotropic conductive adhesive, low temperature soldering, hygrothermal aging, bending tests, reliability

**INTRODUCTION**
Smart tags for fast moving consumer goods is expected to represent a significant portion of the predicted trillion sensors scenario of the future, given that cost and manufacturing volume targets are met. It is not a challenge today to build a well working and highly reliable smart tag with a multitude of functionality given the advanced materials, printing technologies, and hybrid assembly methods available. The challenge is rather to understand where technical compromises can be made, and where they should absolutely be avoided, in order to reach the cost and manufacturing volume targets. The demanded storage times and conditions of a smart tag will probably be relatively short and unproblematic, and the operational lifetime might only be a week or two.

Our main hypothesis is that costs can be cut if the smart tags can be designed to fulfil exactly these needs rather than being over-engineered. Further, we postulate that the ability to control this well is only achievable by understanding the physics of the occurring failures and by issuing related lifetime distributions at various loads. In other words, we believe that costs can be saved during manufacturing of low-cost printed electronics if parts of the rigorous methodologies of high-end products is adapted in a clever manner in the early stages of product development.

In this work, we specifically study a temperature smart tag and the reliability of considered assembly solutions. The tag can measure, evaluate and display or transmit whether a temperature incursion has occurred during the cold transport of temperature sensitive items like food and vaccines. The smart tag is a collection of active and passive discrete electronic components ranging from resistors, capacitors, and transistors assembled on a low cost backplane to enable sensing, evaluation, storage and communication of information. Ideally, full systems would be printed in a continuous manner using a roll-to-toll (R2R) process. However, due to the immaturity of some printed component technology and incompatibility of chemicals used in different processes, printable components are rather manufactured in individual lines and then assembled onto the backplane together with passive components.

Such hybrid integration is highly flexible with respect to changes in design and it enables assembly of known good dies, if inclusion of intermediate testing is considered cost efficient from a yield perspective. However, assembly also introduces a means to failure for the smart tag; components might lose connection both mechanically and electrically due to exposure to bending, heat and humidity during application. Polymers used as adhesives or for protection and metal based routing and connections will degrade over time due to the various environmental loads. In this work we present screening tests performed to evaluate systems for interconnections, comparing an anisotropic conductive adhesive with use of a low temperature solder. The target was to identify critical factors limiting the quality of each

technology. The quality of the joints should not be over-engineered unless accompanied with a particularly low cost. Likewise, reliability should not be placed at risk by selecting solutions resulting in qualities at a borderline level. Commercial tools are applied for studies on R2R hybrid integration relevant for smart tags where thermocompression bonding is performed in a stop-and-go mode with localised heating, e.g. using Datacon 2200 EVO as reported in Ref. [1]; anisotropic conductive adhesives (ACA) was applied in combination with backplanes of PET with screen printed Ag lines. Photonic flash soldering is an alternative R2R-compatible solution with highly localised heating of the regions to be bonded [2]. Application of a standard Sn-Ag-Cu (SAC) solder in combination with backplanes of PET with electroplated Cu lines was feasible since the temperature increase could be limited by controlling the light pulse relative to the geometry and absorption of each material. Traditional reflow, typically performed for such solders at more than 230 °C in a conveyer belt furnace, would otherwise ruin a PET substrate that has a maximum processing temperature in the range 120 – 150 °C.

Detailed reliability studies of hybrid assembly performed using materials and tools relevant for smart tags, are, however, scarce. The performance of interconnects have been observed after environmental exposure like hygrothermal aging and cyclic bending [3,4,5], but tests were either not run to failure or the physics of the observed failures not fully described.

As well explained for both isotropic [6] and anisotropic [7] conductive adhesives, electrical failures in such interconnects are typically not possible to correlate with detectable contact debonding, i.e. a crack. A loss of the local pressure on the conductive particles is expected to be the cause of the failure. Compressive stress is explained to be present in the as-bonded stage primarily due to thermal shrinkage during cool-down after assembly and to some extent due to shrinkage of the matrix material during curing [6] (the contribution of each factor is material dependent). On the other hand, thermal expansion, swelling of the matrix due to water diffusion, and viscoelastic relaxation and creep, are factors reducing the pressure either temporarily or irreversibly. The role of the glass transition temperature (Tg) of the matrix material is in this respect critical; above Tg, the thermal expansion of the matrix material is larger, the creep rates are higher and water is more easily incorporated into the structure. Materials with a low Tg are often weaker cross-linked and have a resulting higher moisture permeability [5]. Incorporation of moisture can lower Tg even further and thereby rendering the system prone to failure due to a lost contact pressure at even lower temperatures [7]. For some matrix materials, like for PET, hydrolysis can occur where the absorbed water molecules open polymer chains resulting in embrittlement [8]. Actual cracks may then form and mechanical, in addition to electrical, connection is lost. The physics behind potential failures is thus a complex combination of processes, also with different time scales, e.g. in the order of minutes for viscoelastic relaxation at elevated temperatures and in the order of hours for swelling caused by moisture [7]. Failures can also occur in the printed silver lines. However, due to the widespread use of RFID technology, this is a relatively more mature technology; lifetime models have been proposed [9], highlighting the importance of the silver material quality.

If a low temperature solder is used instead of an ACA, printed silver lines are commonly replaced by Cu tracks for process compatibility, and laminated rolled Cu is a low cost alternative. Electrical failures in soldered interconnects applied at temperatures well below the melting temperature of the solder are mostly related to formation of regions with intermetallic phases that result in deteriorated mechanical compliance of the joints; above a critical yield stress caused by e.g. thermomechanical or mechanical loading, a crack will form and resistance will increase. Otherwise, moisture is critical with respect to corrosion.

However, for a smart tag that will be employed under rather unchallenging conditions, failures might rather occur in the laminated Cu tracks. From work published in the field of conformable electronics, simulations predict that strain in the tracks is increased for thinner substrates with lower Young's modulus [10]. Experimental work for laminated Cu tracks on PET foils confirmed appearance of micro-cracks and related gradual increase in resistance [11]. The ductility of the Cu will vary with geometries, the rolling process, and possible work hardening taking place during application. Although a smart tag only needs to be bendable and not fully conformable, the principles are relevant. They mention in Ref. [11] that the role of the adhesive used for lamination is probably important, but not well understood.

## EXPERIMENTAL

Test systems representing the two identified technology combinations with potential to meet the cost constraints of the smart tag were designed, fabricated and tested. The aim was to identify critical factors for a minimum required quality of the tags, for each combination. An ACP used in combination with a backplane of PEN with printed silver lines was compared with a low temperature solder used in combination with a backplane of PI or PET with laminated Cu lines.

### Design of test structures

Test samples were designed enabling *in situ* electrical testing of daisy chains of assembled components and reference lines in parallel, see Figure 1. The same design was used for the ACP and the solder. The test samples were oriented along the printing direction because no effect of orientation had been seen in initial studies. The pads were designed for assembly of zero-ohm resistors. The pitch of the test pads was 5.4 mm. The width of the samples was 10.7 mm.

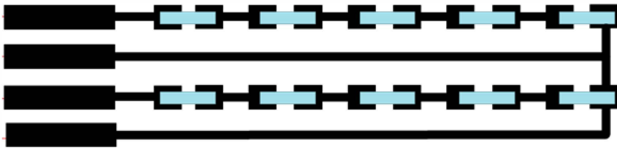

**Figure 1.** Design of test samples employed for *in situ* electrical testing during bending tests and hygrothermal aging, enabling tests of daisy chain and reference lines (black: printed Ag lines; blue: zero-ohm resistors).

**Materials and processing**

For the technology combination with conductive adhesive, a paste from Creative Materials was used, EXP 2647-31, with silver coated glass spheres. The expected Tg is in the range of 50 °C if cured for 2 min at 150 °C according to the provider. The adhesive was used to assemble zero-ohm 0402 resistors onto 4 µm thick silver tracks screen printed onto 125 µm thick PEN foils. Assembly was performed using a pick and place tool exerting a force of 2 N. Curing was performed under a nitrogen atmosphere in a conveyer belt furnace for 9−15 minutes with 130−150 °C as the maximum temperature, without applying any pressure. The material provider recommends a thermode process, but absence of pressure during curing was attempted in order to save cost through an enhanced throughput.

For the technology combination with low temperature solder, Bi-Sn pastes were used. The lowest melting temperature of these alloys is ~138 °C. The solder was stencil printed onto 50 µm thick PI foils and 100 µm thick PET foils, both with 18 µm thick rolled Cu laminated using a layer of adhesive and patterned for routing. The same zero-ohm resistors were assembled as for the system with ACP on PEN backplanes, and reflow was performed under a nitrogen atmosphere in a conveyer belt furnace with 150−170 °C as the maximum temperature.

**Characterization**

Samples were characterized mechanically and electrically as bonded and after different environmental exposures. For several tests, *in situ* electrical testing was performed.

Shear testing was performed using a Nordson DAGE 4000Plus with a shear speed of 10 µm/s and a test height in the range of 20−50 µm. Fracture surfaces were studied using an optical light microscope with extended focus imaging (Olympus BX 60 F5). The mechanically flexible samples were clamped and mechanical supported during shear testing by gluing them onto microscope glass slides with generous amounts of 3M™ Scotch-Weld™ EPX Epoxy Adhesive DP410. Statistical significance of differences observed among sample groups was evaluated using Student's t-tests.

Cross sections of assemblies were studied using a Scanning Electron Microscopy (SEM, FEI Nova NanoSEM 650) and Energy Dispersive X-ray Spectroscopy (EDS, Oxford X-Max50 SDD) in addition to optical microscopy.

Electrical testing of the daisy chains was performed manually using a handheld multimeter, U1252B from Keysight. For *in-situ* measurements during environmental exposures, the samples were attached to a custom-built jig with test probes connected to an Agilent 34970A Data Acquisition Switch Unit via an Agilent 34901A multiplexer card for 4-wire resistance measurements.

Differential scanning calorimetry was performed for the ACP using a DSC 8500 from Perkin Elmer. Heating cycles were run from -50 to 250 °C, ramped at 50 °C/min. Infrared spectroscopy was carried out through attenuated total reflectance FT-IR using a Spectrum One from Perkin Elmer equipped with a universal attenuated total reflection accessory.

**Environmental Exposures**

For the samples with ACP, high temperature storage (HTS) and thermal cycling (TC) was performed in addition to hygrothermal aging (HTA) and bending tests, whereas for the samples with solder, only HTA and bending tests were performed.

**HTS was performed in a Binder heat chamber. TC and HTA were performed in a Sunrise SU250 C climate chamber with *in-situ* electrical characterisation. The temperature was recorded using a K-type thermocouple. The parameter settings applied for the different environmental exposures are presented in**
Table 1.

**Table 1.** Overview of parameter settings for different environmental exposures

| Joint | Substrate | Test | Settings |
|---|---|---|---|
| ACP | PEN | HTS | 120 °C, 20−40% RH* |
| ACP | PEN | TC | -20−100 °C, 120 min cycle |
| ACP | PEN | HTA | 60 °C, 70% RH |
| Solder | PI | HTA | 85 °C, 85% RH |
| Solder | PET | HTA | 85 °C, 85% RH |

* Not controlled

Bending tests were performed using a custom-built test setup consisting of a motorised cylinder with 25 mm radius which rotation is controlled by a digital control unit. The rotation is monitored by an angle-meter and optical switches trigger the changing of rotation direction. The location of the optical switches can be adjusted to make sure all components in the region of interest experience both the straight and bent stages of each cycle.

Samples were aligned and clamped to the cylinder with probes for *in-situ* electrical characterisation. To ensure a constant mechanical tension, controlled weights were hung from the end of each sample. Four PEN and two PI samples failed when applying weights of ~4.2 kg in a static bent tension test whereas too heavy weights for the set-up were needed to reach failure for the PET samples. The increase in resistance was gradual for the samples with ACP on PEN

whereas it was abrupt for the samples with solder on PI. Weights of 1.4 kg was selected for all further tests. This corresponded to a tension (defined as the applied force divided by the cross section area of the substrates) of 10.5 MPa for the PEN, 26.2 MPa for the PI and 13.1 MPa for the PET samples. For simplicity, numbers of cycles were rounded to the nearest thousand.

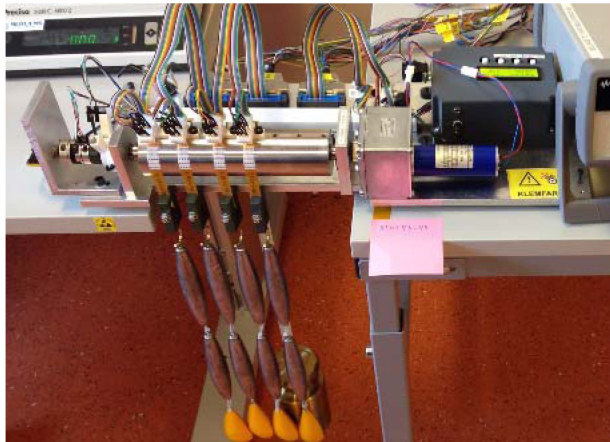

**Figure 2.** Picture of the custom-built test setup for bending tests.

Specifications will vary for each end-user and each specific product, but some 'typical' values were selected as draft specifications for the specific zero-ohm resistors assembled in this work; the test samples should withstand

- at least 720 h (1 month) at 60 °C in 70% RH
- or, 120 h (5 days) at 85 °C in 85% RH
- and, more than 5,000 (one day's test time) cycles of bending with a bending radius of 25 mm and applied weights of 1.4 kg

Electrical failure was defined as a 20% increase in the electrical resistance relative to the value measured initially in each test setup. Mechanical failure was defined as an average fracture load below 0.75 kg for a group of more than five samples. Acceleration factors were estimated assuming an activation energy in the range of 0.7 eV (based on values in Ref. [12] for polymers exposed to humidity). Since the simple Arrhenius relationship could give too conservative estimates, variants of the generalized Eyring relationship, adding the relative humidity as a non-thermal acceleration variable, were also considered [13]. On the other hand, the influence of humidity was largely expected included in the activation energy used.

## RESULTS AND DISCUSSIONS

### ACP on PEN with printed silver lines

Reference silver lines were measured after 72, 144, 216 and 288 h of HTS. Some variation in the resistance values were observed, but any changes were below the defined failure threshold. Even smaller changes were observed for two lines measured after 90, 186 and 282 h of TC, or for two lines measured after 72, 144 and 216 h of HTA. In summary, the printed lines themselves were not considered to fail in the tested intervals.

On the other hand, the resistance of daisy chains, with 10 zero-ohm resistors assembled in series, had multiplied 2−6 times after 72 h of HTS, 2 times after 288 h of TC and 4−6 times after 72 h of HTA. Two or more samples, where assembly had been made using a generous volume of ACP, were measured for each of the electrical results. Clearly, according to our draft specifications, high temperatures, and high temperatures in combination with high humidity, were detrimental for the samples electrically. As the humidity was not controlled during HTS, similar physical effects could play a role in HTS and HTA.

Samples with either the generous or a more standard amount of ACP were prepared for strength tests. A significant increase in bond strength was observed after 288 h of HTS for the samples with generous amounts of ACP (increased from 1.1 to 1.3 kg, 10% standard deviation), and after 282 h of TC for the samples with a smaller amount of ACP (increased from 0.8 to 1.0 kg, 10% standard deviation). The increase in strength was believed to relate to further curing of the matrix material of the ACP. No improvement or degradation in bond strength was observed after 216 h of HTA for either of the sample types. All measured fracture loads of the samples with ACP were above the demanded minimum value and an overview of the shear test results is given in **Error! Reference source not found.**.

Bending tests of two reference silver lines showed no indication of increased resistance even after 35,000 cycles. However, for five test samples with daisy chains, indications of degradations were observed already after a few hundred cycles, and after 4,000 cycles all daisy chains had failed. These were not satisfactory results based on our draft specifications for bending. A continuous increase in resistance was observed for all daisy chains (with slightly different slopes).

Differential scanning calorimetry was performed on samples of the matrix material of the ACP, without the inclusion of particles, and it was confirmed that a full curing was not guaranteed with the applied curing scheme. However, a glass transition temperature in the range 47−51 °C was detected after 15 min curing of a 4 mg sample at 150 °C. According to the provider of the ACP, >40% of the material consists of a thermoplastic polymer and (multiple) diluents. FT-IR analysis indicated that the main thermoplastic polymer was a polyester. A diethylene glycol monoethyl ether acetate diluent was also detected, even after curing.

Cross sectioning and SEM inspection was performed of electrically functional samples after assembly, and of failing samples after HTS. As can be seen in Figure 3, particles of the ACP had apparently been dragged upwards and out of the printed silver lines during the HTS. This could have happened due to diffusion of water into the matrix and resulting swelling. Since polyester chains are subject to hydrolytic ageing, particularly at temperatures above Tg, embrittlement could also explain the observations made; ester hydrolysis leads to chain scissioning that can induce

weaker adhesive properties of the binder [12]. Degradation in bond strength was not observed, which could rule out the role of hydrolysis, but qualitative-wise the joints appeared more brittle when shear tested after HTS, so both swelling and hydrolysis could have been involved.

The results highlight the importance of having a satisfactory curing scheme and a matrix material with a Tg above application temperatures at which high humidity levels can be expected. Compromises in the direction of accepting a partly cured matrix material or a lower Tg to save costs can be highly risky unless HTA tests are successfully passed during qualification. Electrical testing is clearly more important than mechanical testing for an ACP material after, or preferably during, HTA.

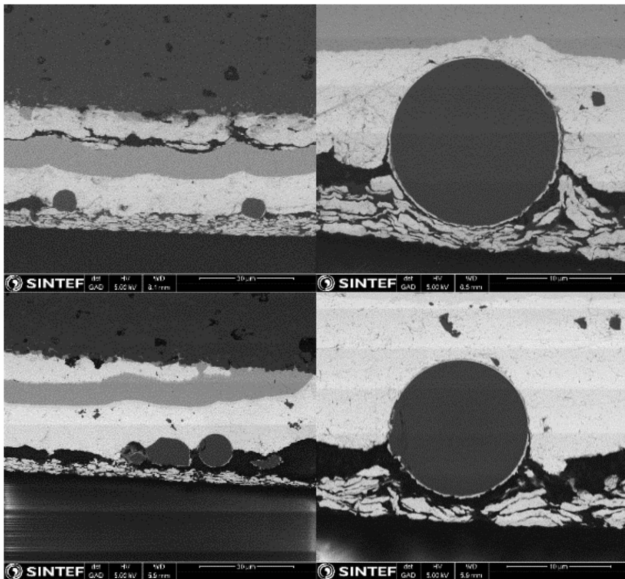


**Figure 3.** SEM images of trapped particles of the ACP (silver-coated silicon oxide spheres) for samples as bonded (upper) and after HTS (lower). The particles have apparently been pulled out of the printed silver line during HTS.

**Bi-Sn solders on PI or PET with Cu-tracks**

Reference Cu lines laminated on PI or PET were exposed to more than 100,000 bending cycles without showing any signs of degradation, indicating a high mechanical reliability of the backplanes themselves.

**A total of 23 PI and six PET samples, each with a daisy chain of 10 soldered zero-ohm resistors, were exposed to bending tests and run to failure. Abrupt failures were seen. Two-parameter Weibull distribution [14] was used to evaluate the results statistically, see**

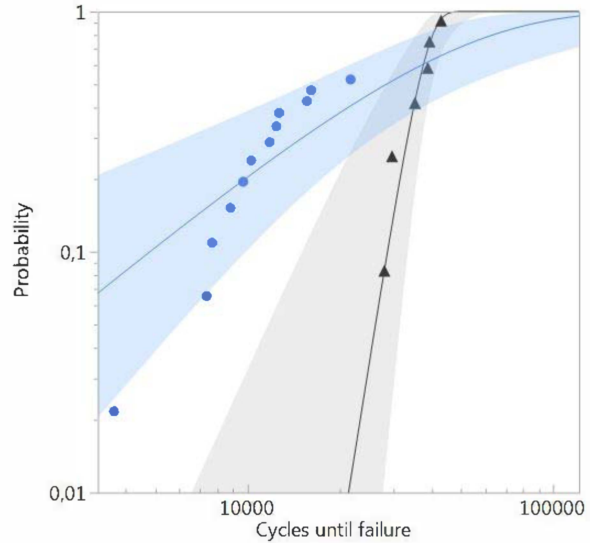


Figure 4. The parameters estimated were α, the characteristic reliability (the number of cycles where 63.2% of the test samples are expected to have failed) and β, the shape parameter (β < 1 indicates early-life failures, β = 1 represents a constant failure rate, and β > 1 often relates to wear-out failures). A value for α of 41,000 cycles and a value for β of 1.1 were estimated for the PI samples (11 out of the 23 samples had not failed when the test was stopped and these were therefore analysed as right censored data). The failures were inspected by cross sectioning the samples and the dominating failure mode was cracks between the solder and the Cu pads. A value for α of 38,000 cycles and a value of β of 8 were estimated for the PET samples. The experiment was repeated with doubled weights for the PI samples, and the dominating failure mode was then observed to shift towards rupture in the Cu tracks near the soldered terminals.

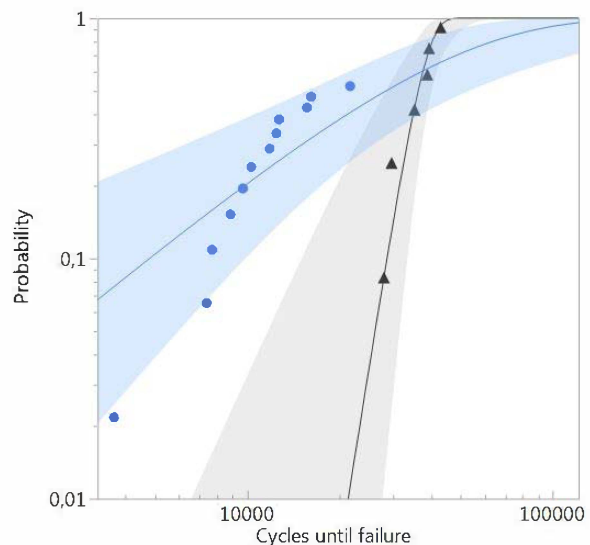


**Figure 4.** Graphical representation of numbers of bending cycles that PI and PET samples sustained before failing electrically (● PI samples, ▲ PET samples).

Shear tests were performed for PI and PET samples as assembled, after HTA, after bending tests, and after combinations thereof. A total of 20−40 samples were measured for each reported fracture load measured after assembly and at least eight samples were measured after various environmental exposures. The standard deviation was in the range of 5−20 %.

As measured after assembly, the fracture load varied between 2.0 and 2.5 kg for the PI samples depending on the applied reflow temperature (150 and 170 °C respectively). By way of comparison, the fracture load was only 1.4 kg for the PET samples (reflowed at 150 °C). Two failure modes were observed, as shown in the upper part of Figure 5. The dominating failure mode, Type I, was cohesive fracture in the adhesive below the Cu tracks. A less frequently observed failure mode, Type II, was cohesive fracture in the solder.

Samples of PI reflowed at 170 °C were exposed to 99 h of HTA, samples of PI reflowed at 150 °C were exposed to 95, 336, 501 and 1000 h of HTA and samples of PET reflowed at 150 °C were exposed to 168 h of HTA, before shear testing. The measured failure loads were 2.4, 2.1, 2.0, 1.9, 1.7 and 1.1 kg, respectively. The three latter values represented statistically significant reductions in strength. Only Type I failure mode was seen after HTA, with three exceptions after 95 h for PI samples reflowed at 150 °C. For the PET samples, as opposed to for the PI samples, the Cu tracks could rather easily be pushed off from the substrate after HTA with a sharp tweezer in their full length, as indicated in the lower part of Figure 5.

Samples of PI reflowed at 170 °C were exposed to 18,000 and 24,000 bending test cycles before shear testing. No electrical failures were seen during the bending tests. Fracture loads of 2.6 and 1.9 kg were measured after the two exposure levels of bending. The former did not represent a statistically significant change from the value measured after assembly whereas the latter represented a degradation.

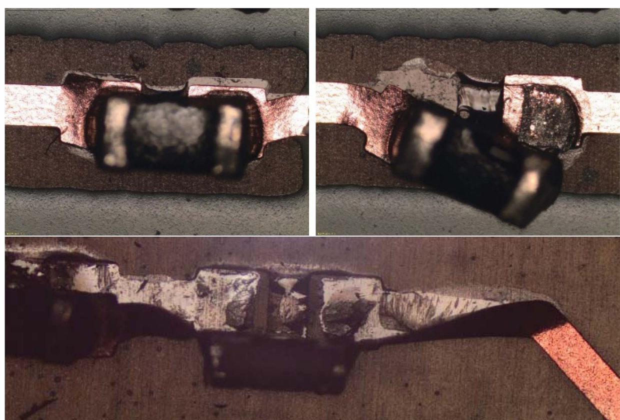

**Figure 5.** Pictures of the two failure modes observed before humidity exposure of solder on PET, cohesive fracture in the adhesive (upper left, Type I) or in the solder (upper right, Type II), and the only failure mode observed afterwards (lower, Type I).

Samples of PI reflowed at 170 °C were exposed to 99 h of HTA followed by 10,000 cycles of bending. The fracture load measured afterwards was 2.4 kg, which did not represent any statistically significant change as compared to as assembled. A mixture of Type I and Type II failure modes was seen.

One PI sample reflowed at 150 °C, with two daisy chains, each consisting of five zero-ohm soldered resistors coupled in series, was measured electrically *in situ* during HTA for 1000 hours without any signs of increase in resistance. Thereafter, the sample was exposed to bending tests where one of the daisy chains failed after 13,000 cycles and the other after 10,000 cycles. The failures were abrupt.

All measured fracture loads of the soldered samples were above the demanded minimum value and an overview of the shear test results is given in **Error! Reference source not found.**.

The observations made for the soldered samples pointed in the direction of the solder joint itself as an uncritical part of the assembly compared to the importance of the quality of the Cu tracks and the material used for the lamination of these. The soldered joints failed only after very high numbers of bending cycles whereas otherwise the Cu tracks ruptured (after bending cycles with a particularly high load) or the weakest interface was the adhesive used for lamination (during shear testing, prominent after HTA). Naturally, this will be different in case of soldering of larger and stiffer components and/or for larger soldered joints, but for smart tags, small components and few and small joints are most relevant.

Some of the considerations made for the matrix material of the ACP with respect to humidity tolerance at high temperatures are therefore relevant also for the soldered system since degradation of the adhesive used for lamination will reduce the mechanical integrity of the Cu tracks. Swelling, hydrolysis (embrittlement, reduced adhesion), and reduction of Tg resulting from exposure to humidity under warm conditions will be critical, although expectedly less than for the described ACP system; the adhesive is only indirectly ensuring electrical continuity. The adhesive used is a bisphenol A epoxy resin for the PI samples whereas it was not known for the PET samples. An epoxy resin is usually considered as more stable than a polyester, but still with some sensitivity to hydrothermal ageing with respect to swelling and/or hydrolysis of the resin.

Although the price difference tends to drop, backplanes of PI, that from our tests appeared to represent more reliable backplanes, are in general more costly than backplanes of PET. A selection must e.g. consider if the possible cost reduction of combining PI with a traditional SAC solder can

outweigh the reduced cost of PET in combination with a Bi-Sn solder. This price scenario is under constant development. Our results indicate that the quality will be more than sufficient for a smart tag choosing any of the tested combinations of backplanes and soldering.

## SUMMARY AND CONCLUSIONS

Based on reliability testing where test samples for smart tags were run to failure and failure analysis was performed, hygrothermal aging was concluded to be most critical both for a system with ACP on PEN with silver tracks and for a system with solder on PI or PET with laminated Cu tracks.

For the system with ACP, it was concluded that a compromise cannot be made with respect to the employed matrix material's resistance to warm and humid conditions, even for an application as a smart tag. Although highly simplified with respect to the complexity of polymers, this translates into a high Tg material for several polymers used as adhesives. On the other hand, for the system with solder, it was concluded that the quality of the lamination of the Cu tracks onto the substrate should be critically evaluated to ensure appropriate reliability of these systems. Sufficient reliability for a smart tag application was demonstrated both for backplanes of PI and PET. Accordingly, the price of the substrates and compatible solders (i.e. both SAC and Bi-Sn for PI and Bi-Sn for PET) can be used as a criterion for selection.

**Table 2.** Overview of measured fracture loads (kg) of differently environmentally exposed samples. Bending cycles are given in kilos of cycles (kc). Results that were statistically significant different from the value measured after assembly (As made), are marked in grey.

| Exposure/ Sample description | As made | 288 h HTS | 282 h TC | 95-216 h HTA | 336 h HTA | 501 h HTA | 1000 h HTA | As made 18 kc | As made 24 kc | 99 h HTA 10 kc |
|---|---|---|---|---|---|---|---|---|---|---|
| PEN, ACP generous | 1.1 | 1.3 | 1.1 | 1.0 | | | | | | |
| PEN, ACP standard | 0.8 | 0.8 | 1.0 | 0.8 | | | | | | |
| PI, at 170 °C | 2.5 | | | 2.4 | | | | 2.6 | 1.9 | 2.4 |
| PI, at 150 °C | 2.0 | | | 2.1 | 2.0 | 1.9 | 1.7 | | | |
| PET, at 150 °C | 1.4 | | | 1.1 | | | | | | |


## ACKNOWLEDGEMENTS

The Research Council of Norway is acknowledged for support through the project 245498/O30 FLEXTAG. We would also like to thank our SINTEF colleagues Joachim Seland Graff and Hanne Opsahl Austad who made valuable contributions to this work.


## REFERENCES


[1] M. Tuomikoski, S. Ihme, A. Huttunen, M. Korkalainen and S. Yrjänä, "Indoor air quality sensing indicators", ESTC 2016

[2] G. Arutinov, J. van den Brand and R. Hendriks, "Photonic Flash Soldering on Flex Foils for Flexible Electronic Systems", 2016 IEEE 66th Electronic Component and Technology Conference

[3] A. Huttunen, T. Happonen and M. Välimäki, "Processing and reliability of bare die LED chip bonding on flexible plastic substrates", ESTC 2016

[4] D.A. van den Ende, R. Hendriks, R. Cauchois, R.H.L. Kusters, M. Cauwe, W.A. Groen and J. van den Brand, "Photonic Flash Soldering of Thin Chips and SMD Components on Foils for Flexible Electronics, IEEE Transactions on Components, Packaging and Manufacturing Technology, Vol. 4, No. 11, Nov 2014.

[5] K. Nagarkar, "Reliability of Compliant Electrically Conductive Adhesives for Flexible PV Modules", 15th IEEE ITHERM Conference

[6] R. Dudek, "reliability investigations on conductive adhesive joints with emphasis on the mechanics of the conduction mechanism", IEEE Transactions on Components and Packaging Technologies, Vol. 23, No. 3, Sept 2000

[7] B. Wunderle, C. Kallmayer, H. Walter, T. Braun, B. Michel and H. Reichl, "Lifetime model for flip-chip on flex using anisotropic conductive adhesive under moisture and temperature loading", IEEE 2008

[8] J. Kiilunen and L. Frisk, "Hygrothermal Aging of an ACA Attached PET Flex-on-Board Assembly", IEEE Transactions on Components and Packaging Technologies, Vol. 4, No. 2, Feb 2014

[9] T. Happonen, T. Ritvonen, P. Korhonen, J. Häkkinen and T. Fabritius, "Modeling the Lifetime of Printed Silver Conductors in Cyclic BendingWith the Coffin-Manson Relation", Transactions on Device and Materials Reliability, Vol. 16, No. 1, March 2016

[10] Y.-Y. Hsu, M. Gonzalez, F. Bossuyt, J. Vanfleteren and I. De Wolf, "Polyimide-Enhanced Stretchable Interconnects: Design, Fabrication, and Characterization, IEEE Transactions on Electron Devices, Vol. 58, No. 8, Aug 2011

[11] F. Bossuyt, S. Dunphy, J. Vanfleteren, J. De Baets, K. Pacheco Morillo, and J. Van den Brand, "Plastic Electronics based Conformable Electronic Circuits", ESTC 2012, DOI: 10.1109/ESTC.2012.6542085

[12] V. Bellenger, M. Ganem, B. Mortaigne, J. Verdu, "Lifetime prediction in the hydrolytic aging of polyesters", Polymer Degradation and Stability 1995, 49, 91

[13] L.A. Escobar and W.Q. Meeker, "A Review of Accelerated Test Models", Statist. Sci. Vol. 21, No. 4 (2006), 552-577
[14] M. Ohring, "Reliability and Failure of Electronics Materials and Devices", New York: Academic, 1998